Interference Energy in C–H and C–C Bonds of Saturated Hydrocarbons: Dependence on the Type of Chain and Relationship to Bond Dissociation Energy

ARTICLE *in* THE JOURNAL OF PHYSICAL CHEMISTRY A · APRIL 2013

Impact Factor: 2.69 · DOI: 10.1021/jp4005746 · Source: PubMed

4 AUTHORS:

Francisco Senna Vieira
NIST Boulder Laboratories
4 PUBLICATIONS **20** CITATIONS
SEE PROFILE

Felipe Fantuzzi
Federal University of Rio de Janeiro
13 PUBLICATIONS **34** CITATIONS
SEE PROFILE

Thiago Cardozo
Federal University of Rio de Janeiro
15 PUBLICATIONS **79** CITATIONS
SEE PROFILE

Marco Nascimento
Federal University of Rio de Janeiro
143 PUBLICATIONS **1,914** CITATIONS
SEE PROFILE

THE JOURNAL OF PHYSICAL CHEMISTRY A

Article

pubs.acs.org/JPCA

Interference Energy in C−H and C−C Bonds of Saturated Hydrocarbons: Dependence on the Type of Chain and Relationship to Bond Dissociation Energy

Francisco Senna Vieira, Felipe Fantuzzi, Thiago Messias Cardozo, and Marco Antonio Chaer Nascimento*

Instituto de Química, Universidade Federal do Rio de Janeiro, Rio de Janeiro RJ 21941-590, Bazil

ABSTRACT: Interference energy for C−H and C−C bonds of a set of saturated hydrocarbons is calculated by the generalized product function energy partitioning (GPF-EP) method in order to investigate its sensitivity to the type of chain and also its contribution to the bond dissociation energy. All GPF groups corresponding to chemical bonds are calculated by use of GVB-PP wave functions to ensure the correct description of bond dissociation. The results show that the interference energies are practically the same for all the C−H bonds, presenting only small variations (0.5 kcal.mol^{-1}) due to the structural changes in going from linear to branched and cyclic chains. A similar trend is verified for the C−C bonds, the sole exception being the cyclopropane molecule, for which only the C−C bond exhibits a more significant variation. On the other hand, although the interference energy is quantitatively the most important contribution to the bond dissociation energy (DE), one cannot predict DE only from the bond interference energy. Differences in the dissociation energies of C−C and C−H bonds due to structural changes in the saturated hydrocarbons can be mainly attributed to quasi-classical effects.

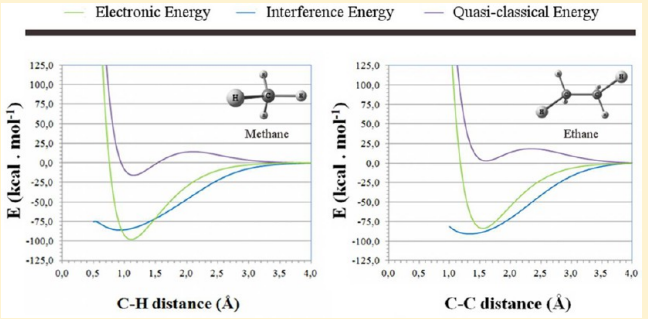

1. INTRODUCTION

Although the chemical bond is usually considered to be a very well established concept in chemistry, its origin and nature are still subject to much discussion and scientific inquiry.[1−14] It is well-known that the minimum in the potential energy surface (PES) responsible for the bond in a stable system is followed by a decrease of potential energy and a rise of kinetic energy, as required by the virial theorem. However, this analysis does not provide a model for explaining bond formation. Since the total kinetic and potential energies are a direct consequence of the form of the total electronic density, the question of why the electronic density of a bonded molecule changes in such a way that results in an energy drop is unanswered by these quantities.[1−3] It is possible to understand the reason why chemical bonds are formed by means of an alternative energy partitioning, derived from density partitioning, in quasi-classical and interference contributions.[1,4,11] This approach shows that the quantum mechanical interference effect promotes a change in the electron density, which is responsible for the energy reduction that leads to the formation of covalent bonds. The results obtained for a variety of diatomic and polyatomic molecules based on this kind of energy partitioning attest that such bonds are formed only in the presence of quantum interference.[3,15−18] It is important to emphasize that the term "quasi-classical" is used in the present context simply to indicate that part of the energy associated with the "quasi-classical" density in the same spirit of Ruedenberg's original work.[11]

There are, however, some important points that remain to be investigated. For example, how sensitive is the interference energy to the chemical environment of the pair of atoms involved in a chemical bond? Also, how is the strength of a chemical bond related to its interference energy? The answers to these and other related questions will be extremely important for establishing the transferability of the interference energy of a given bond to a similar one in a different molecule and to what degree one can estimate the bond energy based solely on the knowledge of its interference energy.

In order to try answering these questions, we propose to examine the interference energy in the C−C and C−H bonds of saturated hydrocarbons. This class of molecules is especially convenient to our purposes since it is experimentally known that most of the properties of those bonds are similar in all members of the series. Also, chemical bonds in saturated hydrocarbons are more amenable to a theoretical investigation than the ones in more complex molecules. In fact, bonding in this class of compounds can be qualitatively well described by traditional Lewis electron pairs. However, there are several important chemical processes in which the breakage of C−C and C−H bonds of saturated hydrocarbons plays an important role, and the activation of these bonds continues to be the subject of recent studies.[19−26]

In previous papers we developed an energy partition scheme, known as the generalized product function energy partitioning method (GPF-EP), and used it to investigate the chemical

Received: January 17, 2013
Revised: April 9, 2013
Published: April 10, 2013

   dx.doi.org/10.1021/jp4005746 | J. Phys. Chem. A 2013, 117, 4025−4034

bond in different classes of molecules.[3,15−18] According to this approach, detailed in section 2, the total energy of the molecule is partitioned into a contribution due to the quantum interference effect and a contribution due to all other effects, collectively referred as to quasi-classical or reference contribution.

In the present work, this partitioning method is used to investigate the sensitivity of the interference energy in C−C and C−H bonds to skeletal changes in saturated hydrocarbons and how the strength of the bonds is related to the interference energies. For this purpose, the interference energies in C−H and C−C bonds for a set of isomeric linear, branched, and cyclic saturated hydrocarbons are analyzed and also compared with experimental dissociation energies. Dissociation scans for C−H and C−C bonds in the simplest saturated hydrocarbons, methane and ethane, are also analyzed in order to evaluate the energy profile in more detail.

2. PARTITIONING OF INTERFERENCE ENERGY AND DENSITY

The method for energy partitioning used herein is called generalized product function energy partitioning (GPF-EP),[4,15] and was derived by applying Ruedenberg's[11] original partitioning scheme to GPF wave functions constructed with modern valence bond group functions. The GPF wave functions have been defined by Li and McWeeny,[29] and their general form is shown in eq 1:

$$\Psi_{\mathrm{GPF}} = \hat{A}[\Psi_1(\vec{r}_1\vec{\omega}_1, \vec{r}_2\vec{\omega}_2, ..., \vec{r}_{N_1}\vec{\omega}_{N_1})\Psi_2(\vec{r}_{N_1+1}\vec{\omega}_{N_1+1}, \vec{r}_{N_1+2}\vec{\omega}_{N_1+2}, ..., \vec{r}_{N_2}\vec{\omega}_{N_2})...] \quad (1)$$

where $\hat{A}$ is the antisymmetrizer operator, indexes 1 and 2 represent different orthogonal wave functions (groups), and r_i and ω_i are electron spatial and spin coordinates, respectively.

Each group is set to be orthogonal to all others, in the same way that generalized valence bond (GVB) pairs are used in the GVB-PP (perfect pairing) wave function. However, in a GPF, groups can be treated with different methods, and more than two electrons can be put in a single group. For saturated systems, the most convenient way to divide such groups is to define one group for each electron pair involved in a chemical bond and a single group for all the electrons belonging to the core. Since core electrons play a smaller role in most chemical bonds, treating them as a single Hartree−Fock (HF) group is a reasonable approximation. In more complex systems, such as aromatic rings, it is necessary to define a group with more than two electrons and carry out the calculations with a full GVB or, equivalently, a spin-coupled wave function.

Only a brief discussion concerning the main aspects of the method will be presented. Detailed information about the method can be found elsewhere in the literature.[4,15]

The reduced density matrices of first and second order (RDM-1 and RDM-2) for GPF wave functions are as follows:

$$\rho(\vec{r}_1, \vec{r}_1') = \sum_{\mu=1}^{\eta} \rho^{\mu}(\vec{r}_1, \vec{r}_1') \quad (2)$$

$$\pi(\vec{r}_1\vec{r}_2) = \sum_{\mu=1}^{\eta} \pi^{\mu}(\vec{r}_1\vec{r}_2) + \frac{1}{2}\sum_{\eta}^{\mu=1}\sum_{\eta}^{\nu>\mu}\left[\rho^{\mu}(\vec{r}_1)\rho^{\nu}(\vec{r}_2) - \frac{1}{2}\rho^{\mu}(\vec{r}_2, \vec{r}_1)\rho^{\nu}(\vec{r}_1, \vec{r}_2)\right] \quad (3)$$

where η is the number of groups in the GPF function. The total electronic energy expression for a GPF wave function in terms of the reduced density matrices is

$$E_{\mathrm{GPF}} = \sum_{\mu=1}^{\eta}\left\{\int [\hat{h}\rho^{\mu}(\vec{r}_1, \vec{r}_1')]_{\vec{r}_1=\vec{r}_1'}\, d\vec{r}_1 + \frac{1}{2}\int \frac{\pi^{\mu}(\vec{r}_1, \vec{r}_2)}{r_{12}} d\vec{r}_1\, d\vec{r}_2\right\} + \frac{1}{2}\sum_{\mu=1}^{\eta}\sum_{\nu\neq\mu}^{\eta}\left\{\frac{1}{2}\int \frac{\rho^{\mu}(\vec{r}_1)\rho^{\nu}(\vec{r}_2)}{r_{12}} d\vec{r}_1 d\vec{r}_2\right\} - \frac{1}{2}\sum_{\mu=1}^{\eta}\sum_{\nu\neq\mu}^{\eta}\left\{\frac{1}{4}\int \frac{\rho^{\mu}(\vec{r}_2, \vec{r}_1)\rho^{\nu}(\vec{r}_1, \vec{r}_2)}{r_{12}} d\vec{r}_1 d\vec{r}_2\right\} + \sum_{A=1}^{M}\sum_{B>A}^{M}\frac{Z_A Z_B}{r_{AB}} \quad (4)$$

where $\hat{h}$ is the one-electron operator, which includes both kinetic energy and electron−nuclei potential energy, and r_{12} is the interelectronic distance. The expression found in the first term in braces stands for the intragroup energy, and the remaining part of the equation stands for the coulomb and exchange intergroup contributions, respectively. The GPF-EP method separates both ρ and π into interference and reference densities, the latter meaning the sum of quasi-classical densities. For instance, the interference and quasi-classical densities for a single group are

$$\rho_{\mathrm{I}}{}^{\mu}(\vec{r}_1) = \sum_{r,s}^{N^{\mu}}{}' \langle r, s\rangle^{\mu} p(r|s) \quad (5)$$

$$\rho_{\mathrm{QC}}{}^{\mu}(\vec{r}_1) = \sum_{r=1}^{N^{\mu}} [\phi_r^{\mu}(\vec{r}_1)]^2 \quad (6)$$

where μ is the selected group index, N^{μ} is the number of electrons in this group, $p(r|s)$ are the density matrix elements expressed in the orbital basis set, and $\langle r,s\rangle^{\mu}$ is the interference density for orbitals ϕ_r and ϕ_s:

$$\langle r, s\rangle^{\mu} = \phi_r^{\mu}(\vec{r})\phi_s^{\mu}(\vec{r}) - \frac{1}{2}\xi(r, s)\{[\phi_r^{\mu}(\vec{r})]^2 + [\phi_s^{\mu}(\vec{r})]^2\} \quad (7)$$

where $\xi(r,s)$ is the overlap integral between $\phi_r{}^{\mu}$ and $\phi_s{}^{\mu}$. Thus, the total energy of the system can be separated as follows:

$$E[\mathrm{tot}] = E[\mathrm{ref}] + E[\mathrm{I}] + E[\mathrm{II}] + E[\mathrm{x}] \quad (8)$$

where E[ref] is the total reference energy; E[I] and E[II] are the first- and second-order interference energies, respectively; and E[x] is the total intergroup exchange energy, which arises from the antisymmetrization of the GPF wave function. It is important to emphasize that the E[x] term would not exist if the GPF wave function consisted of a single group. Consequently, the exchange term represents merely a symmetry correction to the reference energy and arises only because of the separation of the total wave function into different groups. Thus, the choice of the number of groups and the number of electrons in each group must be done with caution, since the results in terms of energy partition and its interpretation will strongly rely on the quality of this selection.

The reference and first-order interference energies can be further separated into kinetic (T[ref] and T[I]), electron−electron potential (V_{ee}[ref] and V_{ee}[I]), and electron−nuclei (V_{en}[ref] and V_{en}[I]) energies. The second-order interference

dx.doi.org/10.1021/jp4005746 | J. Phys. Chem. A 2013, 117, 4025−4034

energy $E[\mathrm{II}]$ consists exclusively of electron−electron repulsion terms and can be equivalently referred to as $V_{ee}[\mathrm{II}]$. These contributions can also be divided into intragroup and intergroup contributions as follows:

$$E[\mathrm{ref}] = \sum_{\mu=1}^{\eta} E^{\mu}[\mathrm{ref}] + \sum_{\mu<\nu}^{\eta} E^{\mu,\nu}[\mathrm{ref}] \tag{9}$$

$$E[\mathrm{I}] = \sum_{\mu=1}^{\eta} E^{\mu}[\mathrm{I}] \tag{10}$$

$$E[\mathrm{II}] = \sum_{\mu=1}^{\eta} E^{\mu}[\mathrm{II}] + \sum_{\mu<\nu}^{\eta} E^{\mu,\nu}[\mathrm{II}] \tag{11}$$

$$E[\mathrm{X}] = \sum_{\mu<\nu}^{\eta} E^{\mu,\nu}[\mathrm{ref}] \tag{12}$$

3. COMPUTATIONAL DETAILS

The calculations were carried out by use of GPF functions, with all core electrons taken as one group and each electron pair corresponding to a chemical bond put in a different group. The core group is treated with the RHF method and the remaining groups with the GVB-PP method. This has been the general approach in calculations involving the GPF-EP method, and so far has led to the most interesting results.

A basis set analysis, up to quintuple basis sets, has been carried out in previous papers dealing with diatomic and small polyatomic molecules.[15,16] These studies have shown that the interference energy is the least sensitive among the quantities obtained in the energy partitioning, while the reference and exchange contributions are the most sensitive, to the quality of the basis set. However, the results also showed that a correct description of the energy partitioning can be obtained even with basis sets of modest size containing polarization functions. On the basis of these results, and considering the size of the molecules to be examined, the 6-31G** and cc-pVDZ[27] basis sets were used in all the present calculations.

First, energy partitioning was performed for molecules at their equilibrium geometry. The geometry optimizations were carried out at the GVB-PP level by use of the program Jaguar 7.6.[28] After the geometry optimization, both the GPF wave function for the molecule and the energy partition were obtained. A version of the VB2000[29] code modified by our group was used in order to perform the GPF-EP partition. The number of Jacobi rotations between electron groups during the self-consistent field procedure was set to 5 to obtain better convergence.

In order to analyze the changes in energy contributions as C−H and C−C bonds are formed, geometry scans were performed by carrying out a geometry optimization at selected frozen values of the coordinate chosen for the scan. The scans were performed until no significant changes in the total energy (below 1 kcal·mol^{-1}) were noticeable, yielding for both bonds a superior limit of 4.00 Å .Thus, the dissociations of the C−H in methane bond and the C−C bond in ethane ranged from 0.50 to 4.00 Å and from 1.00 to 4.00 Å, respectively, with of steps of 0.02 Å. At each point, the GPF wave functions were calculated and the energy was partitioned. Correlation contributions were estimated at the left-eigenstate completely renormalized coupled-cluster [CR-CC(2,3)] level, with cc-pVDZ basis set, for both equilibrium and dissociated geometries.[31−33] The enthalpy at 298 K was also calculated at those points, at the GVB-PP level.

4. ENERGY PARTITIONING AT EQUILIBRIUM GEOMETRY

To investigate how sensitive the interference energy is to structural changes around a given bond, a series of small saturated hydrocarbons was considered. In this series we have included linear, cyclic, and branched species up to six carbon atoms, as seen in Table 1.

Table 1. List of Hydrocarbons Calculated

acyclic hydrocarbons	cyclic hydrocarbons
CH_4	C_3H_6
C_2H_6	C_4H_8
C_3H_8	C_5H_{10}
C_4H_{10} (methylpropane)	C_6H_{12}
C_4H_{10} (*n*-butane)	
C_5H_{12} (pentane)	
C_5H_{12} (neopentane)	
C_6H_{14} (hexane)	

Figure 1A shows that the values of the total interference energy are practically the same for all the C−H bonds, presenting only small variations (0.5 kcal·mol^{-1}) due to structural changes in going from linear to branched and cyclic chains. A similar trend can be verified for the C−C bonds. The sole exception is observed in the cyclopropane molecule, for which the C−C bond exhibits a more significant variation. Therefore, the GPF-EP partition scheme results are consistent with the known properties of these bonds and the obtained interference energies can be taken as characteristic values of C−H and C−C bonds in these classes of compounds.

As noticed, the value of the interference energy for the C−C bond in cyclopropane (∼−88 kcal·mol^{-1}) is smaller than those typical for the other C−C bonds (∼−92 kcal·mol^{-1}). A decrease in the interference energy, although considerably smaller, can also be observed in other less tensioned rings, such as cyclobutane and cyclopentane. The contributions to the interference energy for cyclopropane are slightly different from those of the other cyclic molecules: $V_{en}[\mathrm{I}]$ is 6 kcal·mol^{-1} higher, $V_{ee}[\mathrm{I}]$ is 6 kcal·mol^{-1} lower, and $T[\mathrm{I}]$ is 2 kcal·mol^{-1} higher (Figure 1B,C). The reasons for this behavior are better understood by comparing the bonding orbitals of the different cyclic hydrocarbons (Figure 2) and by looking at the changes in density promoted by interference between the orbitals involved in the C−C bonds, also referred to as "interference densities" (Figure 3).

From Figure 2, one can see that, in order to preserve orthogonality between orbitals in different orbital pairs, the singlet coupled lobe orbitals of the C−C bonds of cyclopropane are not oriented along the C−C bond axis. Consequently, the overlap between each pair is reduced, compared to the C−C bonds of the other saturated hydrocarbons. As can be seen in Figure 3, this decrease in the overlap affects the interference density, which presents its maximum value displaced from the bond axis. Thus, the interference profile obtained for cyclopropane is found to be consistent with the peculiar properties of the C−C bonds in this compound.

Similarly to what was observed for all the other studied molecules, for all hydrocarbons and for both types of bonds, the most important contribution responsible for lowering the total

dx.doi.org/10.1021/jp4005746 | J. Phys. Chem. A 2013, 117, 4025−4034

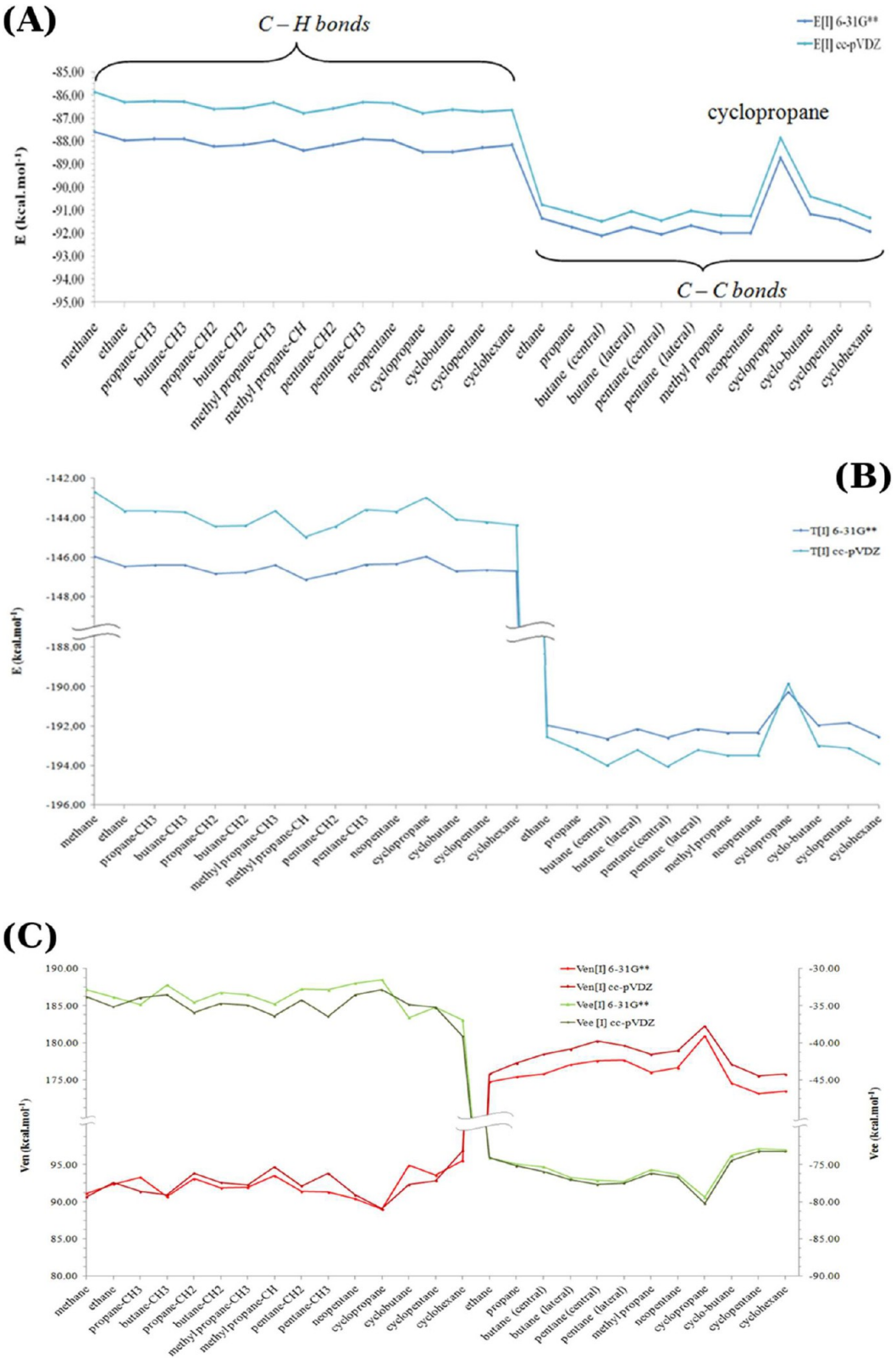

Figure 1. (A) Interference energies, (B) kinetic interference energies, and (C) potential interference energies for C−H and C−C bonds.

energy is the interference kinetic energy (Figure 1B). It is noteworthy that the components of the total interference energy, $T[I]$, $V_{en}[I]$, and $V_{ee}[I]$, follow the same general behavior, with $T[I]$ being the most negative and $V_{en}[I]$ presenting a positive sign. This result is in agreement with the mechanism for bond formation first proposed by Ruedenberg.[11] We also point out that these results are independent of the basis set chosen (Figure 1), though interference energies are slightly smaller for the cc-pVDZ basis set.

Second-order interference values for specific groups are all on the order of 10^{-2} kcal·mol^{-1} and, therefore, will not be further

dx.doi.org/10.1021/jp4005746 | J. Phys. Chem. A 2013, 117, 4025−4034

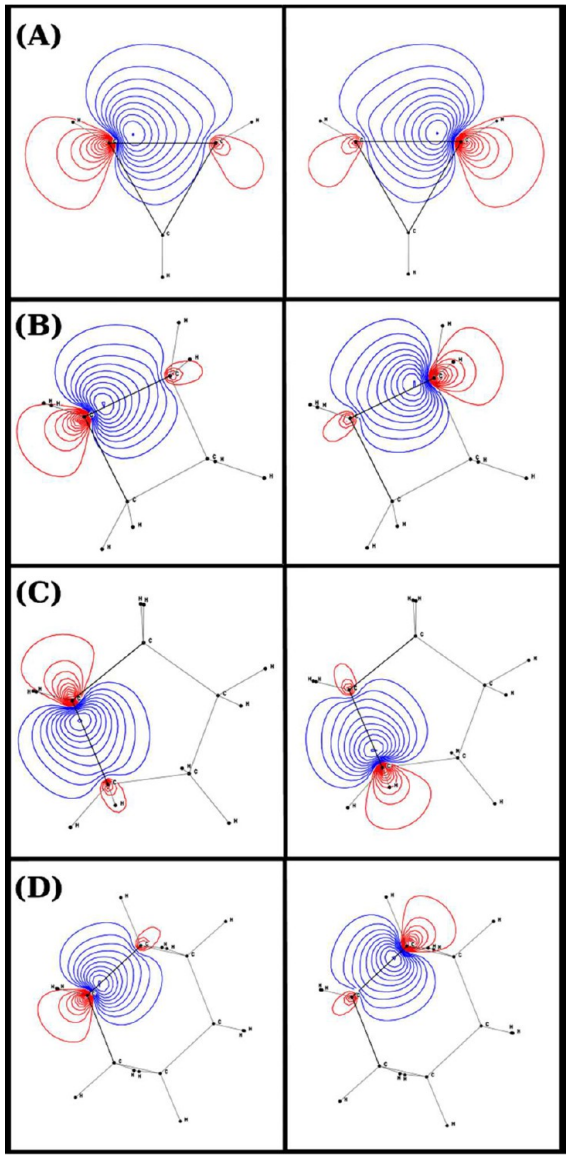

Figure 2. GVB-PP orbitals for the C−C bonds of each cyclic hydrocarbon studied, with cc-pVDZ basis set: (A) cyclopropane; (B) cyclobutane; (C) cyclopentane; (D) cyclohexane.

considered in the discussion. Also, since the reference energies do not vanish as the atoms are set apart, their absolute values at equilibrium geometries are irrelevant to our analysis and therefore need not be presented.

A first test of the transferability of bond interference energies can be made with the assumption that $E[I]$ of the alkane molecule can be obtained by summing the $E[I]$ contributions of its individual bonds. For this purpose, we took the standard $E[I]_{C-H}$ equal to a fourth of the total $E[I]$ of methane (−85.87 kcal·mol^{-1}) and the standard $E[I]_{C-C}$ (−90.77 kcal·mol^{-1}) from the ethane molecule. Figure 4 shows an excellent correlation between calculated $E[I]$ values and the ones assuming transferability of the bonds $E[I]$. Of course, the sum of individual bond contributions to $E[I]$ will be equal for all molecules with the same number of C−C and C−H bonds (for example, methylpropane and *n*-butane). These results are a clear indication that this procedure can be used to obtain reliable $E[I]$ values for larger molecules of saturated hydrocarbons. It is noteworthy that, even for the cyclopropane

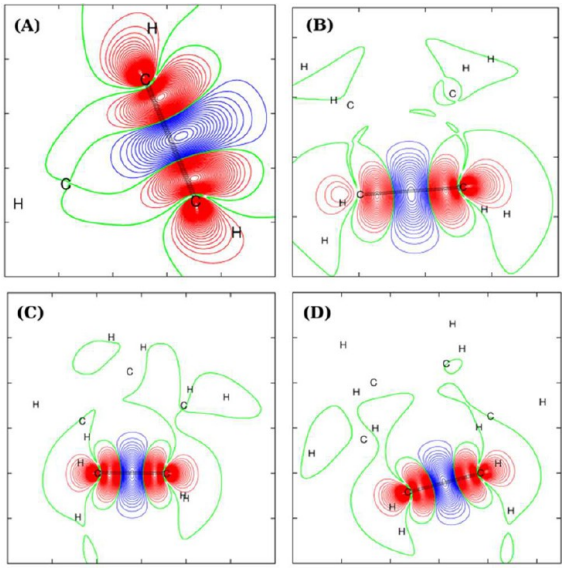

Figure 3. Interference density contour diagrams for the studied cyclic hydrocarbons, plotted in a spatial cut section parallel to the plane of each bond. Green, blue, and red lines correspond to zero, positive, and negative interference densities, respectively. Incremental values between the lines are equal to 0.001 V^{-1}. ρ_{min} = −0.035 V^{-1}, ρ_{max} = +0.017 V^{-1}. (A) Cyclopropane; (B) cyclobutane; (C) cyclopentane; (D) cyclohexane.

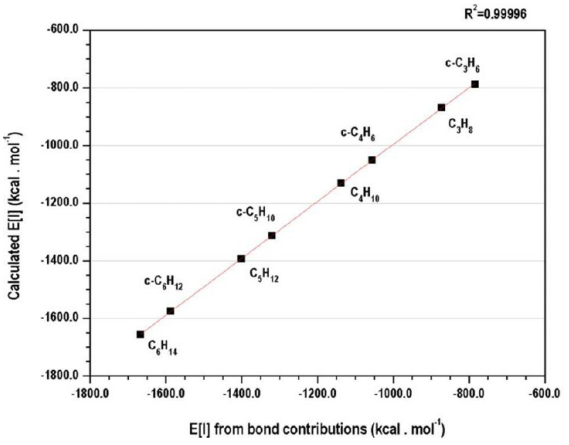

Figure 4. Transferability of bond interference energy: comparison between calculated $E[I]$ values and the ones obtained from individual $E[I]$ bond contributions.

molecule, the $E[I]$ value is accurately predicted by this method. Since its $E[I]$ contribution is composed mostly by C−H bonds, it is not surprising that the anomalous $E[I]$ value of the C−C bond does not affect the analysis significantly.

5. ENERGY PARTITIONING ALONG THE BOND DISSOCIATION PROCESS

When the calculated interference energy magnitudes are compared with experimental dissociation energies (Figure 5), it is clear that the bond interference energy is quantitatively the most important contribution in all cases considered. It can also be noticed that interference contributions are larger than the respective dissociation energies for C−C bonds, while the opposite occurs for C−H bonds. The fact that the interference energy is greater for homonuclear bonds was expected, since the interference energy components tend to increase with the

dx.doi.org/10.1021/jp4005746 | J. Phys. Chem. A 2013, 117, 4025−4034

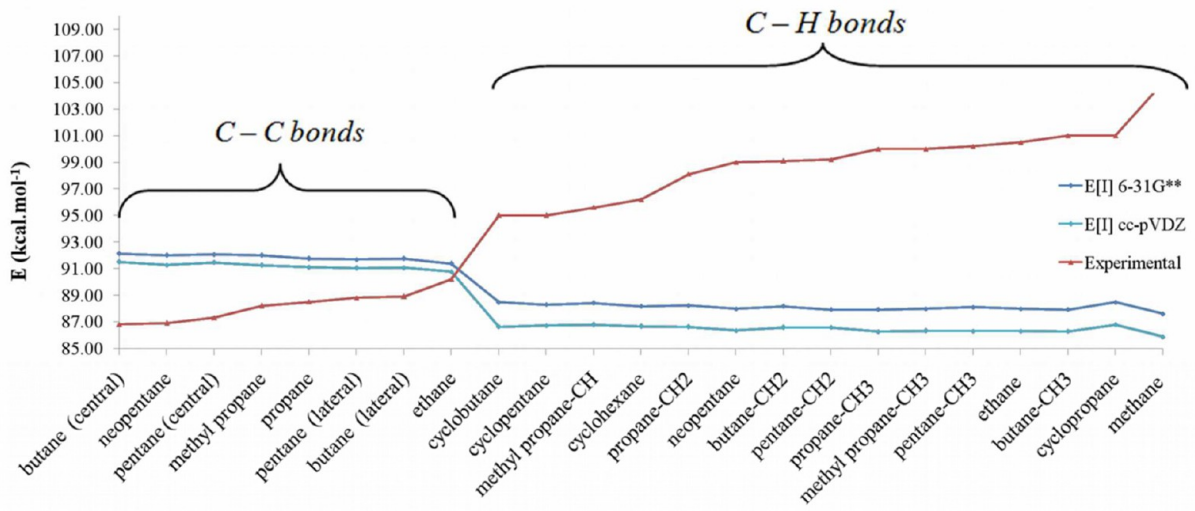

Figure 5. Interference energies and experimental dissociation energies data.[34].

overlap between orbitals involved in bonding. However, it is also clear that one cannot predict dissociation energies only from interference contributions since the differences between dissociation energies of the bonds are considerably larger than the differences between corresponding interference energies (Figure 5). Three other contributions must be considered to account for this difference, namely, electron correlation, the zero-point energy, and the change in the symmetry-corrected quasi-classical energy, ΔE[ref + x]. From these three contributions, the one that can be more directly separated in terms of bonds is ΔE[ref + x] and one can expect it to be smaller for the C−C bonds, since all C−C bond dissociation energies are quite close to their respective interference energies (Figure 5). In fact, by analyzing the energy partitioning toward the dissociation of C−H and C−C bonds of methane and ethane, respectively, it becomes clear that the E[ref + x] term slightly contributes to the potential well in the PES of the C−H bond, while in the C−C dissociation of ethane this term actually destabilizes the bonded system. The energy partitioning of both dissociations will be further discussed in the next sections.

Since the quasi-classical part of the energy appears to be of utmost importance in the description of the processes of bond breaking and bond formation, we next quantify its contribution by applying GPF-EP to several points along the bond dissociation path. We also estimate the magnitude of the electronic correlation energy and the zero-point energy at the equilibrium geometry and for the dissociated molecule.

Bond dissociation calculations were performed for the C−C bond in ethane and the C−H bond in methane according to the procedure described in section 3. In these calculations, all contributions to the total energy have been set to zero at the largest value of the bond distance considered in the scans (4.00 Å), since the main interest is on relative contributions.

Although GVB wave functions might be a qualitatively accurate way to describe the bonds in the studied systems, they do not take into account the breakage of the electrons' singlet coupling. Naturally, this restriction will generate dissociation energies slightly different than expected. Calculations for the isolated dissociation products in the triplet state, however, have shown that such differences are very small and, for the purposes of this discussion, may be deemed irrelevant.

5.1. Methane. Figure 6 shows a potential energy surface along the C−H bond dissociation path in methane, together

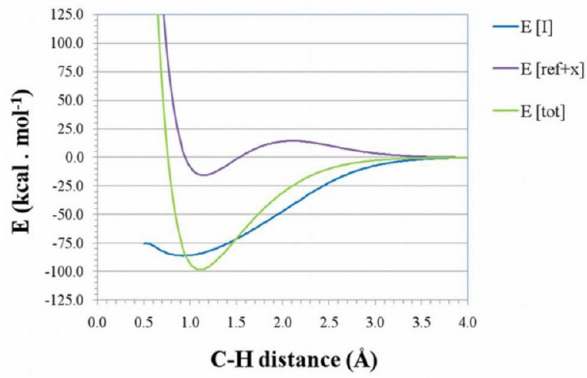

Figure 6. Energy profiles for dissociation of the C−H bond in methane.

with total first-order interference energies (E[I]) and total symmetry-corrected quasi-classical energy (E[ref + x]). The second-order interference contribution has been neglected because it is very small (∼0.5 kcal·mol^{-1}) and practically constant along the whole path. The first important point to be noticed is that first-order interference contribution is considerably larger than all other contributions at the minimum of the potential well (E[I] = −85.6 kcal·mol^{-1} and E[ref + x] = −15.0 kcal·mol^{-1} at 1.10 Å). Since the exchange energy is merely a symmetry correction to the pair density, the figure actually represents the C−H bond energy profile within the symmetry-corrected quasi-classical approximation, compared to the interference energy profile.

From Figure 6 it is seen that the minimum in the interference energy surface occurs at a C−H distance (0.88 Å) considerably smaller than that of equilibrium (1.10 Å) and is very shallow. On the other hand, the minimum in the reference energy surface occurs at a distance (1.20 Å) closer to the equilibrium internuclear distance and is more pronounced. It is clear that even though the purely quantum-mechanical contributions are predominantly responsible for formation of the potential well, the actual position of the PES minimum is strongly influenced by quasi-classical effects.

dx.doi.org/10.1021/jp4005746 | J. Phys. Chem. A 2013, 117, 4025−4034

It is also noteworthy, from Figure 6, that the shape of the quasi-classical curve presents a very subtle maximum at 2.12 Å. Thus, in the absence of interference, not only would the potential well be very shallow (15.0 kcal·mol^{-1}) but also an energy barrier would arise in this dissociation. This barrier in the quasi-classical energy arises from the conformational changes that follow the dissociation. On the other hand, the interference energy always decreases from 4.00 to 1.10 Å, reassuring the fact that interference is exclusively related to bond formation/breakage processes. Such behavior is consistent with the system evaluated: a single bond is broken during the $CH_4 \rightarrow CH_3 + H$ reaction.

The components of the interference energy (T[I], V_{en}[I], and V_{ee}[I]) are shown in Figure 7A, just for the C−H bond,

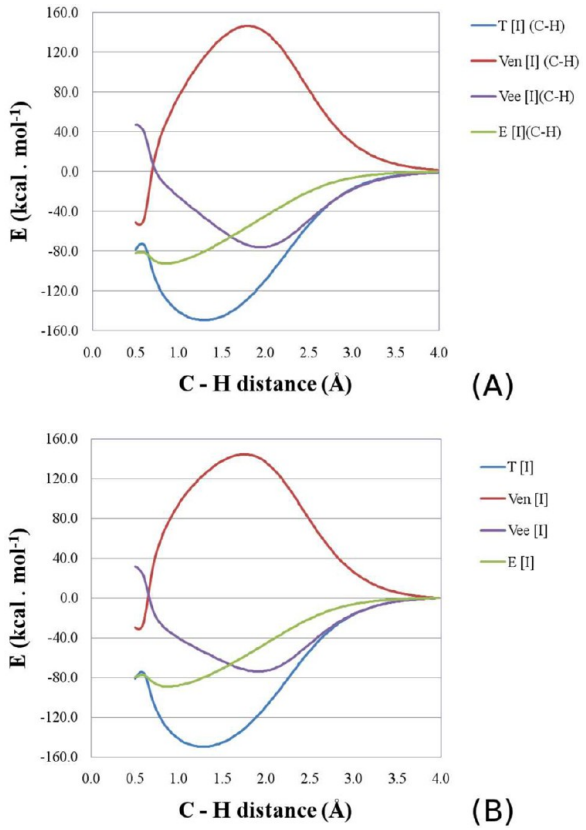

Figure 7. Interference profiles along the C−H bond dissociation, (A) for the C−H bond and (B) for the whole molecule. Basis set: 6-31G**.

and for the whole molecule in Figure 7B. For the sake of comparison, the interference contributions for all groups were set to 0 at 4.00 Å. The fact that these figures are nearly identical is not surprising as it just reflects that the changes in interference energy are much more pronounced in the group involved in bond formation or breaking. The differences in the interference energy for the remaining groups are so small that they are barely noticeable, except for a small change in the shape of the V_{en}[I] curve. As should be clear by now, the same fundamental mechanism for bond formation found for other molecules,[15−18] where interference changes to the density promote a reduction of the kinetic energy and an increase of the potential energy, is also present here. We emphasize that these changes are relative to a quasi-classical (interference-free) reference density, and that, obviously, the total kinetic energy increases as the total potential energy decreases, as per the virial theorem.

In Table 2 we present the main energy differences between the dissociated and bonded CH_4, including the enthalpy at 298 K and an estimate of correlation energy with the CR-CC(2,3) method. It is clear that those remaining contributions play only a minor role in the appearance of the potential well in the PES compared to the interference contributions, confirming the previous discussion.

Table 2. Energy Differences between Dissociated and Bonded CH_4[a]

component	method	ΔE, kcal·mol^{-1} (4.00−1.10 Å)
E_{total}	GVB-PP	98.2
E_{total}	CR-CC(2,3)	107.0
E_{corr}[b]		8.9
E[I + II][c]	GVB-PP	83.1
E[ref + x]	GVB-PP	15.0
ZPE	GVB-PP	−9.6
$H_{298\ K}$	GVB-PP	89.9
H_{298K}	exp	105.0

[a]Basis set: cc-pVDZ. [b]Correlation energy: $E_{CR\text{-}CC(2,3)} - E_{GVB\text{-}PP}$. [c]Sum of first- and second-order interference energies.

In Figure 8 we present the interference densities calculated at four points along the C−H dissociation path. At the equilibrium geometry (1.10 Å), the profile is consistent with our previous observation: a large increase in electronic density is promoted by the interference effect at the interatomic axis. Also, the maximum of the interference density is not centered between the carbon and hydrogen atoms, being rather displaced toward hydrogen. As the atoms become closer

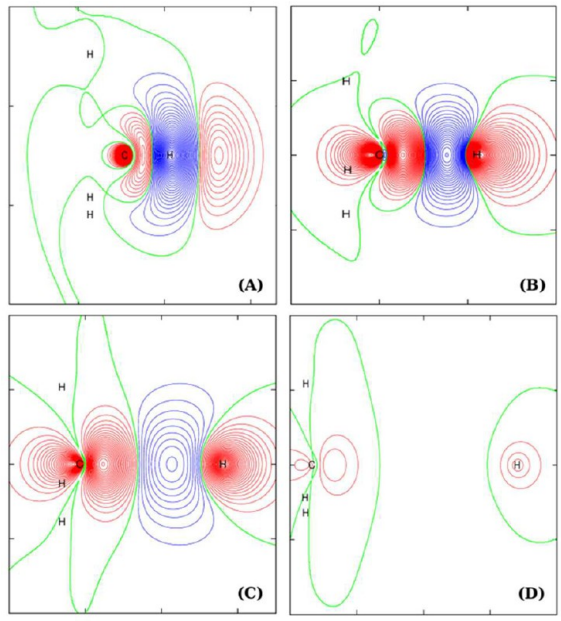

Figure 8. Interference density contour diagrams for dissociation of the C−H bond in methane, plotted in a spatial cut section parallel to the plane of the bond. Incremental values between the lines are equal to 0.001 V^{-1}. C−H distances and contour values: (A) d = 0.76 Å, ρ_{min} = −0.159 V^{-1}, ρ_{max} = +0.032 V^{-1}; (B) d = 1.10 Å, ρ_{min} = −0.035 V^{-1}, ρ_{max} = +0.021 V^{-1}; (C) d = 1.88 Å, ρ_{min} = −0.003 V^{-1}, ρ_{max} = +0.009 V^{-1}; (D) d = 3.08 Å, ρ_{min} = −0.003 V^{-1}, ρ_{max} = +0.000 V^{-1}.

dx.doi.org/10.1021/jp4005746 | J. Phys. Chem. A 2013, 117, 4025−4034

(0.76 Å), such maximum is actually centered at the hydrogen nucleus, decreasing electronic density in the internuclear region. Such behavior is also consistent with the energy profile, since $E[\mathrm{I}]$ increases at small bond distances. On the other hand, separation of the atoms leads to the complete disappearance of interference densities, just as expected.

5.2. Ethane (C−C Bond). Similar calculations were carried out for C−C bond dissociation in ethane. Figure 9 shows the

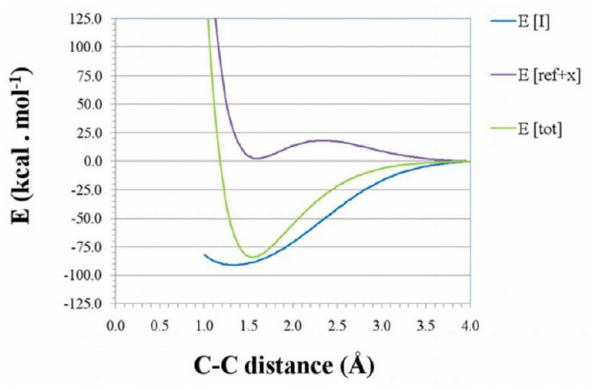

Figure 9. Energy profiles for dissociation of the C−C bond in ethane.

potential energy surface for ethane along the C−C dissociation path together with the curves for $E[\mathrm{I}]$ and $E[\mathrm{ref} + \mathrm{x}]$. Again, the $E[\mathrm{II}]$ contribution is very small and constant along the whole path and is therefore neglected. In this case, the interference energy contribution is not only the sole contributor to bond formation but also surpasses slightly the total energy ($E[\mathrm{I}]$ = −88.9 kcal·mol^{-1} and $E[\mathrm{tot}]$ = −85.2 kcal·mol^{-1}, both at 1.54 Å). This profile is different from that obtained for methane and is also consistent with our previous comparison of interference energies and bond dissociation energies. The quasi-classical contribution $E[\mathrm{ref} + \mathrm{x}]$ presents a minimum value of 1.2 kcal·mol^{-1} at a C−C distance very close to that of equilibrium, showing that the carbon−carbon bond would not be formed in the quasi-classical approximation in spite of the fact that the actual position of the PES minimum is influenced by quasi-classical effects.

In Figure 10 we show the different contributions to the interference energy along the C−C dissociation path just for the C−C bond (Figure 10A) and for the whole molecule (Figure 10B). The qualitative aspect of the $E[\mathrm{I}]$ surface is the same in both figures, but the changes in its components are more pronounced than those observed for the C−H bond in methane. This is a simple consequence of the presence of a greater number of electron groups. Nevertheless, it is evident that the interference energy variations are mostly related to bond-formation or bond-breaking processes.

In Table 3 we present correlation and enthalpy estimates for both equilibrium and dissociated geometries of C_2H_6 dissociation. Once again, those contributions seem to play a minor role in the bond-breaking process.

In Figure 11, we present contour plots for changes in the electronic density promoted by the quantum-mechanical interference effect. It is clear that interference effect promotes a large increase in electronic density at the internuclear region. At equilibrium distance (1.54 Å), the interference density presents its maximum precisely at the middle of the bond. As the atoms are brought together (1.0 Å), this maximum remains at this central position, in contrast to the behavior previously

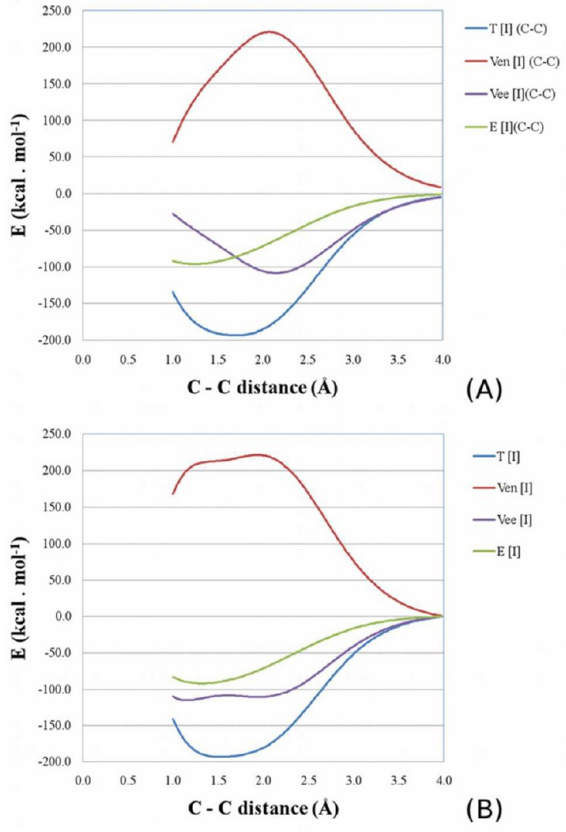

Figure 10. Interference profiles along the C−C bond dissociation, (A) for the C−C bond and (B) for the whole molecule. Basis set: 6-31G**.

Table 3. Energy Differences between Dissociated and Bonded C_2H_6[a]

component	method	ΔE, kcal·mol^{-1} (4.00−1.54 Å)
E_{total}	GVB-PP	83.8
E_{total}	CR-CC(2,3)	95.6
E_{corr}[b]		11.8
$E[\mathrm{I} + \mathrm{II}]$[c]	GVB-PP	87.1
$E[\mathrm{ref} + \mathrm{x}]$	GVB-PP	−3.3
ZPE	GVB-PP	−9.8
$H_{298\mathrm{K}}$	GVB-PP	76.7
$H_{298\mathrm{K}}$	exp	90.2

[a]Basis set: cc-pVDZ. [b]Correlation energy: $E_{\mathrm{CR\text{-}CC(2,3)}} - E_{\mathrm{GVB\text{-}PP}}$. [c]Sum of first- and second-order interference energies.

observed for C−H bond interference density. This is expected due to the symmetric nature of the C−C bond. Interestingly, compressing the atoms beyond the internuclear equilibrium distance causes the appearance of two new interference density maxima near each nucleus. At larger distances, interference densities vanish, as expected for the reasons previously discussed.

6. CONCLUSIONS

In this work, the sensitivity of the interference energy to small structural variations was evaluated for a set of saturated hydrocarbons. The results show that the interference energies are practically the same for all the C−H bonds, presenting only small variations (0.5 kcal·mol^{-1}) due to the structural changes in going from linear to branched and cyclic chains. A similar

dx.doi.org/10.1021/jp4005746 | J. Phys. Chem. A 2013, 117, 4025−4034

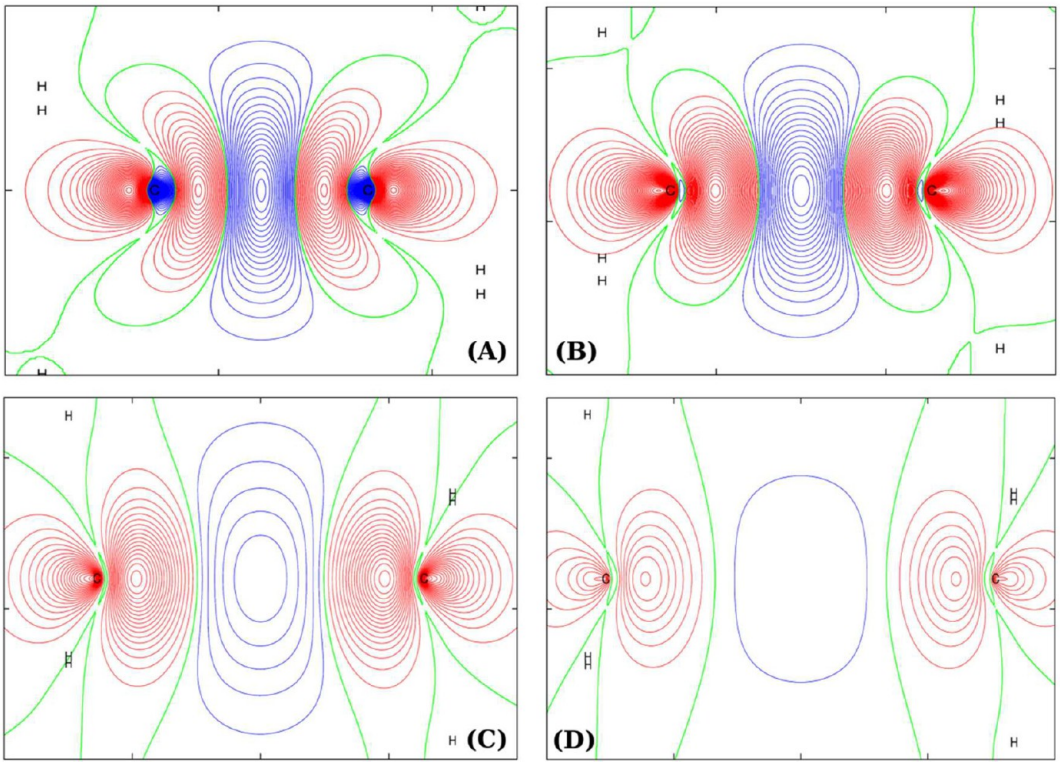

Figure 11. Interference density contour diagrams for dissociation of the C−C bond in ethane, plotted in a spatial cut section parallel to the plane of the bond. Incremental values between the lines are equal to 0.001 V^{-1}. C−C distances and contour values: (A) d = 1.00 Å, ρ_{min} = −0.028 V^{-1}, ρ_{max} = +0.052 V^{-1}; (B) d = 1.54 Å, ρ_{min} = −0.031 V^{-1}, ρ_{max} = +0.017 V^{-1}; (C) d = 2.54 Å, ρ_{min} = −0.023 V^{-1}, ρ_{max} = +0.005 V^{-1}; (D) d = 3.07 Å, ρ_{min} = −0.007 V^{-1}, ρ_{max} = +0.001 V^{-1}.

trend is verified for the C−C bonds, the sole exception being the cyclopropane molecule, for which only the C−C bond exhibits a more significant variation. The GPF-EP partition scheme results are, therefore, consistent with the known properties of these bonds and the obtained interference energies can be taken as characteristic values of C−H and C−C bonds in these classes of compounds.

The comparison between experimental bond dissociation energies and interference energies shows that the differences in bond dissociation energies are much greater than one could predict simply by analyzing the interference contribution. Quasi-classical, correlation, and zero-point contributions are mainly responsible for the changes observed in those dissociation energies and are clearly more sensitive than interference to those structural modifications.

By analyzing the energy profiles calculated for dissociations of the C−C bond in ethane and the C−H bond in methane, it becomes clear that both bonds are formed due to interference effects between orbitals participating in the bond. Also, the electronic density profile reveals that the interference effect is responsible for concentrating electronic density in the internuclear region. These results, along with the observation that the interference energy of a bond is quantitatively the most important contribution to its dissociation energy, reiterate the conclusions reported in previous works: that chemical bonds would not be formed in the absence of interference.[4,15−18] However, in spite of being the main factor that contributes to bond formation, interference energy alone does not account for the differences found in the dissociation energy of very similar bonds, such as those investigated herein.

AUTHOR INFORMATION

Corresponding Author

*E-mail chaer01@gmail.com; phone +55-21-2562-7563; fax +55-21-2562-7265.

Notes

The authors declare no competing financial interest.

ACKNOWLEDGMENTS

We acknowledge FAPERJ, CAPES and CNPq for financial support.

REFERENCES

(1) Nascimento, M. A. C. The Nature of the Chemical Bond. *J. Braz. Chem. Soc.* **2008**, *19*, 245−256.
(2) Wilson, C. W.; Goddard, W. A. Exchange Kinetic Energy, Contragradience, and Chemical Binding. *Chem. Phys. Lett.* **1970**, *5*, 45−49.
(3) Kutzelnigg, W. The Physical Origin of the Chemical Bond. In *Theoretical Models of Chemical Binding*; Maksic, Z. B., Ed.; Springer-Verlag: Heidelberg, Germany, 1990; Vol. *2*, p 1.
(4) Cardozo, T. M. A Ligação Química como um Fenômeno de Interferência. Ph.D. Thesis, 2009.
(5) Woon, D. E.; Dunning, T. H. Theory of Hypervalency: Recoupled Pair Bonding in SF_n (n = 1−6). *J. Phys. Chem. A* **2009**, *113*, 7915−7926.
(6) Bader, R. F. W. Definition of Molecular Structure: By Choice or by Appeal to Observation? *J. Phys. Chem. A* **2010**, *114*, 7431−7444.
(7) Ponec, R.; Cooper, D. L. Anatomy of Bond Formation. Bond Length Dependence of the Extent of Electron Sharing in Chemical Bonds from the Analysis of Domain-Averaged Fermi Holes. *Faraday Discuss.* **2007**, *135*, 31−42.

(8) Ponec, R.; Cooper, D. L. Anatomy of Bond Formation. Domain-Averaged Fermi Holes as a Tool for the Study of the Nature of the Chemical Bonding in Li_2, Li_4, and F_2. *J. Phys. Chem. A* **2007**, *111*, 11294−11301.
(9) Vidal, I.; Melchor, S.; Dobado, J. On the Nature of Metal−Carbon Bonding: AIM and ELF Analyses of MCH_n (n = 1−3) Compounds Containing Early Transition Metals. *J. Phys. Chem. A* **2005**, *109*, 7500−7508.
(10) Pilme, J.; Silvi, B. Comparative Study of the Bonding in the First Series of Transition Metal 1:1 Complexes M−L (M = Sc, ..., Cu; L = CO, N_2, C_2H_2, CN^-, NH_3, H_2O, and F^-). *J. Phys. Chem. A* **2005**, *109*, 10028−10037.
(11) Ruedenberg, K. The Physical Nature of the Chemical Bond. *Rev. Mod. Phys.* **1962**, *34*, 326−376.
(12) Bitter, T.; Wang, S. G.; Ruedenberg, K.; Schwarz, W. H. E. Toward a Physical Understanding of Electron-Sharing Two-Center Bonds. II. A Pseudo-Potential Based Approach. *Theor. Chim. Acta* **2010**, *127*, 237−257.
(13) Bitter, T.; Ruedenberg, K.; Schwarz, W. H. E. Toward a Physical Understanding of Electron-Sharing Two-Center Bonds. I. General Aspects. *J. Comput. Chem.* **2007**, *28*, 411−422.
(14) Ruedenberg, K.; Schmidt, M. W. Physical Understanding through Variational Reasoning: Electron Sharing and Covalent Bonding. *J. Phys. Chem. A* **2009**, *113*, 1954−1968.
(15) Cardozo, T. M.; Nascimento, M. A. C. Energy Partitioning for Generalized Product Functions: the Interference Contribution to the Energy of Generalized Valence Bond and Spin Coupled Wave Functions. *J. Chem. Phys.* **2009**, *130*, No. 104102.
(16) Cardozo, T. M.; Nascimento, M. A. C. Chemical Bonding in the N_2 Molecule and the Role of the Quantum Mechanical Interference Effect. *J. Phys. Chem. A* **2009**, *113*, 12541−12548.
(17) Cardozo, T. M.; Nascimento Freitas, G.; Nascimento, M. A. C. Interference Effect and the Nature of the π-Bonding in 1,3-Butadiene. *J. Phys. Chem. A* **2010**, *114*, 8798−8805.
(18) Fantuzzi, F.; Cardozo, T. M.; Nascimento, M. A. C. The Role of Quantum-Mechanical Interference and Quasi-Classical Effects in Conjugated Hydrocarbons. *Phys. Chem. Chem. Phys.* **2012**, *14*, 5479−5488.
(19) Hunter, K. C.; East, A. L. L. Properties of C−C Bonds in *n*-Alkanes: Relevance to Cracking Mechanisms. *J. Phys. Chem A* **2002**, *106*, 1346−1356.
(20) Jun, C.-H. Transition Metal-Catalyzed Carbon-Carbon Bond Activation. *Chem. Soc. Rev.* **2004**, *33*, 610−618.
(21) Matsuda, T.; Tsuboi, T.; Murakami, M. Rhodium-Catalyzed Carbonylation of Spiropentanes. *J. Am. Chem. Soc.* **2007**, *129*, 12596−12597.
(22) Rybtchinski, B.; Oevers, S.; Montag, M.; Vigalok, A.; Rozenberg, H.; Martin, J. M.; Milstein, D. Comparison of Steric and Electronic Requirements for C-C and C-H Bond Activation. Chelating vs Nonchelating Case. *J. Am. Chem. Soc.* **2001**, *123*, 9064−9077.
(23) Hu, X.; Li, H.; Wu, T. Approaching and Bond Breaking Energies in the C-H Activation and Their Application in Catalyst Design. *J. Phys. Chem. A* **2011**, *115*, 904−910.
(24) Labinger, J. A.; Bercaw, J. E. Understanding and Exploiting C-H Bond Activation. *Nature* **2002**, *417*, 507−514.
(25) Bergman, R. G. Organometallic Chemistry: C-H Activation. *Nature* **2007**, *446*, 391−393.
(26) Lersch, M.; Tilset, M. Mechanistic Aspects of C-H Activation by Pt Complexes. *Chem. Rev.* **2005**, *105*, 2471−2526.
(27) Dunning, T. H. Gaussian Basis Sets for Use in Correlated Molecular Calculations. I. The Atoms Boron Through Neon and Hydrogen. *J. Chem. Phys.* **1989**, *90*, 1007−1023.
(28) Jaguar, version 7.6. Schrödinger LLC, New York, 2009.
(29) Li, J.; McWeeny, R. VB2000: Pushing Valence Bond Theory to New Limits. *Int. J. Quantum Chem.* **2002**, *89*, 208−216.
(30) Schmidt, M. W.; Baldridge, K. K.; Boatz, J. A.; Elbert, S. T.; Gordon, M. S.; Jensen, J. H.; Koseki, S.; Matsunaga, N.; Nguyen, K. A.; Shyjun, S. U.; et al. General Atomic and Molecular Electronic Structure System. *J. Comput. Chem.* **1993**, *14*, 1347−1363.
(31) Piecuch, P.; Włoch, M. Renormalized Coupled-Cluster Methods Exploiting Left Eigenstates of the Similarity-Transformed Hamiltonian. *J. Chem. Phys.* **2005**, *123*, No. 224105.
(32) Piecuch, P.; Gour, J. R.; Włoch, M. Left-Eigenstate Completely Renormalized Equation-of-Motion Coupled-Cluster Methods: Review of Key Concepts, Extension to Excited States of Open-Shell Systems, and Comparison with Electron-Attached and Ionized Approaches. *Int. J. Quantum Chem.* **2009**, *109*, 3268−3304.
(33) Ge, Y.; Gordon, M. S.; Piecuch, P. Breaking Bonds With the Left Eigenstate Completely Renormalized Coupled-Cluster Method. *J. Chem. Phys.* **2007**, *127*, 174106−6.
(34) Luo, Y. R. *Handbook of Bond Dissociation Energies in Organic Compounds*; CRC Press: Boca Raton, FL, 2003.